

UNCLASSIFIED

AD NUMBER
ADB282896
NEW LIMITATION CHANGE
TO Approved for public release, distribution unlimited
FROM Distribution authorized to U.S. Gov't. agencies only; Proprietary Info.; Aug 2001. Other requests shall be referred to U.S. Army Medical Research and Materiel Command, 504 Scott St., Ft. Detrick, MD 21702-5012.
AUTHORITY
USAMRMC ltr, dtd 28 July 2003

THIS PAGE IS UNCLASSIFIED

AD _____

Award Number: DAMD17-99-1-9329

TITLE: Integration of Digital Detectors into a Diffraction
Enhanced Imaging System

PRINCIPAL INVESTIGATOR: Miklos Kiss
Dr. Dale Sayers

CONTRACTING ORGANIZATION: North Carolina State University
Raleigh, North Carolina 27695

REPORT DATE: August 2001

TYPE OF REPORT: Annual Summary

PREPARED FOR: U.S. Army Medical Research and Materiel Command
Fort Detrick, Maryland 21702-5012

DISTRIBUTION STATEMENT: Distribution authorized to U.S. Government
agencies only (proprietary information, Aug 01). Other requests
for this document shall be referred to U.S. Army Medical Research
and Materiel Command, 504 Scott Street, Fort Detrick, Maryland
21702-5012.

The views, opinions and/or findings contained in this report are
those of the author(s) and should not be construed as an official
Department of the Army position, policy or decision unless so
designated by other documentation.

20021001 031

NOTICE

USING GOVERNMENT DRAWINGS, SPECIFICATIONS, OR OTHER DATA INCLUDED IN THIS DOCUMENT FOR ANY PURPOSE OTHER THAN GOVERNMENT PROCUREMENT DOES NOT IN ANY WAY OBLIGATE THE U.S. GOVERNMENT. THE FACT THAT THE GOVERNMENT FORMULATED OR SUPPLIED THE DRAWINGS, SPECIFICATIONS, OR OTHER DATA DOES NOT LICENSE THE HOLDER OR ANY OTHER PERSON OR CORPORATION; OR CONVEY ANY RIGHTS OR PERMISSION TO MANUFACTURE, USE, OR SELL ANY PATENTED INVENTION THAT MAY RELATE TO THEM.

LIMITED RIGHTS LEGEND

Award Number: DAMD17-99-1-9329
Organization: North Carolina State University

Those portions of the technical data contained in this report marked as limited rights data shall not, without the written permission of the above contractor, be (a) released or disclosed outside the government, (b) used by the Government for manufacture or, in the case of computer software documentation, for preparing the same or similar computer software, or (c) used by a party other than the Government, except that the Government may release or disclose technical data to persons outside the Government, or permit the use of technical data by such persons, if (i) such release, disclosure, or use is necessary for emergency repair or overhaul or (ii) is a release or disclosure of technical data (other than detailed manufacturing or process data) to, or use of such data by, a foreign government that is in the interest of the Government and is required for evaluational or informational purposes, provided in either case that such release, disclosure or use is made subject to a prohibition that the person to whom the data is released or disclosed may not further use, release or disclose such data, and the contractor or subcontractor or subcontractor asserting the restriction is notified of such release, disclosure or use. This legend, together with the indications of the portions of this data which are subject to such limitations, shall be included on any reproduction hereof which includes any part of the portions subject to such limitations.

THIS TECHNICAL REPORT HAS BEEN REVIEWED AND IS APPROVED FOR PUBLICATION.

Carole B. Christian

6/4/07

REPORT DOCUMENTATION PAGEForm Approved
OMB No. 074-0188

Public reporting burden for this collection of information is estimated to average 1 hour per response, including the time for reviewing instructions, searching existing data sources, gathering and maintaining the data needed, and completing and reviewing this collection of information. Send comments regarding this burden estimate or any other aspect of this collection of information, including suggestions for reducing this burden to Washington Headquarters Services, Directorate for Information Operations and Reports, 1215 Jefferson Davis Highway, Suite 1204, Arlington, VA 22202-4302, and to the Office of Management and Budget, Paperwork Reduction Project (0704-0188), Washington, DC 20503

1. AGENCY USE ONLY (Leave blank)		2. REPORT DATE August 2001	3. REPORT TYPE AND DATES COVERED Annual Summary (1 Aug 00 - 31 Jul 01)	
4. TITLE AND SUBTITLE Integration of Digital Dectectors into a Diffraction Enhanced Imaging System			5. FUNDING NUMBERS DAMD17-99-1-9329	
6. AUTHOR(S) Miklos Kiss Dr. Dale Sayers				
7. PERFORMING ORGANIZATION NAME(S) AND ADDRESS(ES) North Carolina State University Raleigh, North Carolina 27695 E-Mail: mzkiss@unity.ncsu.edu			8. PERFORMING ORGANIZATION REPORT NUMBER	
9. SPONSORING / MONITORING AGENCY NAME(S) AND ADDRESS(ES) U.S. Army Medical Research and Materiel Command Fort Detrick, Maryland 21702-5012			10. SPONSORING / MONITORING AGENCY REPORT NUMBER	
11. SUPPLEMENTARY NOTES				
12a. DISTRIBUTION / AVAILABILITY STATEMENT Distribution authorized to U.S. Government agencies only (proprietary information, Aug 01). Other requests for this document shall be referred to U.S. Army Medical Research and Materiel Command, 504 Scott Street, Fort Detrick, Maryland 21702-5012.				12b. DISTRIBUTION CODE
13. ABSTRACT (Maximum 200 Words) <p>Refraction contrast of cylindrical objects have been obtained using Diffraction Enhanced Imaging (DEI) and compared to the conventional radiographic contrast. Lucite cylinders and nylon wires were imaged using 18 keV synchrotron radiation at the National Synchrotron Light Source (NSLS) at Brookhaven National Laboratory. The DEI images were obtained by placing a Silicon analyzer crystal tuned to the [333] plane in the beam path between the sample and the detector. They showed improved contrast of the objects when compared to normal radiographs. This comparison, called the gain value, is the ratio of the refraction contrast (or peak contrast) to the conventional radiographic contrast. Experiments and computer simulation consistently resulted of gain values larger than one, indicating improved contrast due to DEI. Experimental results and corresponding computer simulations are presented.</p>				
14. SUBJECT TERMS Diffraction Enhanced Imaging, Radiographic Contrast, Refraction Contrast				15. NUMBER OF PAGES 11
				16. PRICE CODE
17. SECURITY CLASSIFICATION OF REPORT Unclassified	18. SECURITY CLASSIFICATION OF THIS PAGE Unclassified	19. SECURITY CLASSIFICATION OF ABSTRACT Unclassified	20. LIMITATION OF ABSTRACT Unlimited	

Table of Contents

Cover	
SF298	2
Table of Contents	3
Introduction	4
Annual Summary	4
Experimental Setup and Methods	4
Discussion of Results	5
Training Accomplishments	9
Key Research Accomplishments	9
Reportable Outcomes	9
Conclusions	10
References	10

Introduction

Refraction contrast of simple objects have been obtained using Diffraction Enhanced Imaging (DEI) [1, 3] and compared to conventional radiographic contrast. Lucite cylinders and nylon wires were imaged using 18 keV synchrotron radiation at the National Synchrotron Light Source (NSLS) at Brookhaven National Laboratory. The DEI images were obtained by placing a silicon analyzer crystal tuned to the [333] plane in the beam path between the sample and the detector. They showed improved contrast of the objects when compared to normal radiographs. This comparison, called the DEI gain, is the ratio of the refraction contrast (or peak contrast) to the conventional radiographic contrast. Experiments and computer simulation consistently resulted of gain values larger than one, indicating much higher contrast levels due to DEI. This is part of an ongoing effort to develop a clinical DEI prototype for mammography. One of the challenges in developing the prototype is choosing an optimal digital detector for integration into the system. The recent successes of DEI (and phase contrast imaging, a related technique) in showing improved contrast of spiculations and lesions in breast tissue [2, 4, 5, 6] has inspired similar studies to determine the contrast of calcifications. An important factor in the choice of detector is the ability to resolve pixel-sized or near-pixel-sized objects.

The objects imaged in this study were chosen because of their simple geometry and well-characterized physical properties (e.g., refractive index, attenuation coefficient, density). The objects ranged in size from 2.54 cm down to 100 μm , which is close to the size of a detector pixel. A computer model simulating DEI images of these objects has also been developed and its results have been compared to experimental results.

Annual Summary

Experimental Setup and Methods

Experiments were carried out at the X-15A beamline, a general-purpose beamline at the National Synchrotron Light Source, Brookhaven National Laboratory, Upton, New York. A diagram of the apparatus is shown in figure 1.

The apparatus consisted of a double crystal Bragg monochromator that prepared an imaging beam of 1-mm height and 8-cm width. Images were obtained at 18 keV. The imaging beam was monitored by an ionization chamber to measure the skin entry dose to the various phantoms. Plastic absorbers were used to control the dose to the phantoms. A fast shutter system was used to control the exposure to the detector. The shutter opened when the scanning stage was at a constant velocity and was closed at the end of the scan range before the stage was slowed to a stop. The dose was controlled by a combination of incident beam Lucite absorbers and the scanning speed. For DEI images, an additional silicon [333] analyzer crystal was placed in the beam path between the sample and the detector. The analyzer was tuned by rotating it about its horizontal axis. A second ionization chamber measured the exit dose and the image was recorded using a Fuji HR5 image plate. The plates were read out using a Fuji BAS2500 Image Plate Reader.

Conventional radiographs were obtained by placing the image plate on the sample stage, perpendicular to the beam (as seen in Figure 1a), and scanning the sample and plate together through the beam. DEI images were obtained by scanning the sample and the image plate in opposite directions. Raw images were obtained with the analyzer crystal tuned to the Bragg angle (peak images), or on either side of the Bragg peak at angles corresponding the full-width half-maximum (FWHM) value of the rocking curve. Figure 2 shows the rocking curve profile

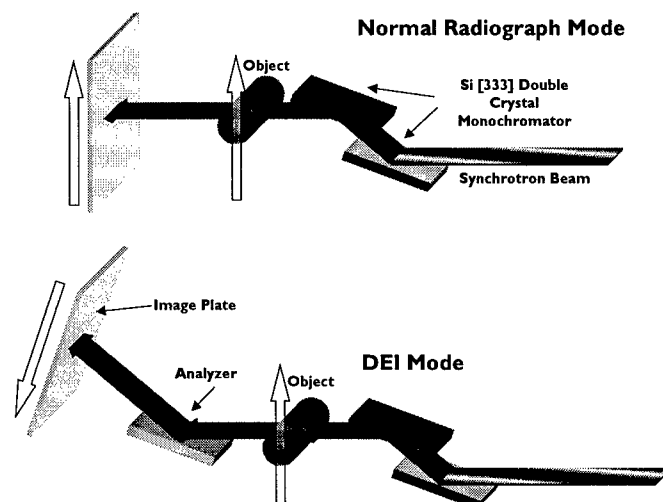


Figure 1. Diagram of apparatus used to acquire images at the X15A beamline at NSLS. Image is not to scale. a) Conventional radiograph mode, b) DEI mode.

for the analyzer crystal tuned to the [333] plane at 18 keV. The FWHM value for silicon [333] at 18 keV is approximately $3.6 \mu\text{radians}$. Images of a sample taken with the analyzer crystal tuned to either side of the peak are also shown.

In order to characterize the contrast of small objects imaged using DEI, samples were chosen which had a simple geometry and well-known physical characteristics. This study will eventually include images and analysis of actual calcifications in breast tissue, but they are not included here. So, wires and cylinders of various composition and diameters were chosen. Table 1 lists the objects imaged and their respective diameters.

Table 1. Characteristics of samples used for imaging.

Object	Diameters
Lucite cylinder	2.54 cm, 1.27 cm, 0.635 cm
Nylon fishing line	0.7112 mm, 0.5588 mm, 0.2032 mm, 0.101 mm

Modeling the DEI images by computer was accomplished by tracing an x-ray through the object using Snell's law to track changes in direction of the x-ray at both the entrance and exit from the object, and the exponential attenuation law to calculate the amount of radiation attenuated by the object along the path. The simulation also accounted for a finite source and finite detector by convolving the image of the object with a simulated source profile and simulated detector profile. Details for the source were obtained from the NSLS, while details for the detector were obtained from previous experiments (as outlined in the 2000 Annual Report). Characteristics of the detector included its PSF and noise levels.

Discussion of Results

Figure 3 shows experimental images of the Lucite cylinders and the Nylon wires. The refraction image is a composite of the images taken at either side of the rocking curve and combined according to the following relation:

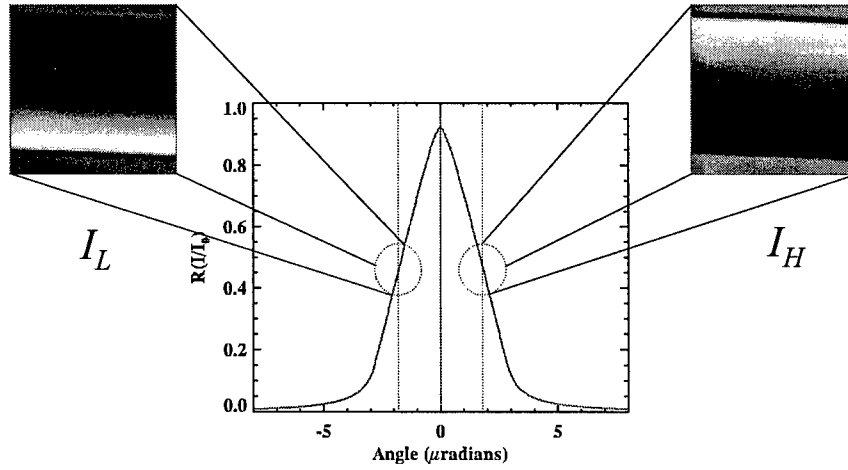


Figure 2. Rocking curve profile for the [333] plane of the analyzer crystal at 18 keV. The angle of zero denotes the Bragg diffraction angle. The images labeled IL and IH are of a Lucite cylinder 1.27 cm in diameter. It is important to note how the images seem reverses of each other.

$$\Delta\theta_z = \frac{I_H R(\theta_L) - I_L R(\theta_H)}{I_L \left. \frac{dR}{d\theta} \right|_{\theta_H} - I_H \left. \frac{dR}{d\theta} \right|_{\theta_L}}, \quad (1)$$

where I_H and I_L are the radiation intensities of the images taken on the high-angle and low-angle sides of the rocking curve, respectively. $R(\theta_H)$ and $R(\theta_L)$ are the reflectivities of the rocking curve on the respective sides and $dR/d\theta$ are the first derivatives of the rocking curve at the respective angles. The term $\Delta\theta_z$ is applied on a pixel-by-pixel basis. Thus in the figure it is clear that larger objects tend to show up in images with roughly the same intensity when comparing DEI to a normal radiograph. In other words, they have approximately the same contrast. As the objects get smaller, the radiographs tend to degrade while the DEI images (both refraction and peak) boast a much higher contrast. In fact, for the 0.101 mm Nylon wire, the object is not visible in the image, while the corresponding DEI images show the object. This is an important point because the pixel size is 50 μm , just half the diameter of the wire. The point spread function (PSF) of the Fuji Image Plate reader is about 160 μm . This is a significant factor in a DEI system's ability to detect pixel-sized and near-pixel-sized calcifications.

Contrast was determined by measuring values for the minimum, maximum and/or background from several vertical line profiles in each image. The radiographic contrast is defined by,

$$C_{rad} = \frac{I_{avg} - I_{min,rad}}{I_{avg}}, \quad (2)$$

where I_{avg} is the average background in the image, and I_{min} is the minimum value in the object. The peak contrast is given by,

$$C_{peak} = \frac{I_{avg} - I_{min,peak}}{I_{avg}}, \quad (3)$$

with similar definitions as in equation 2. The main difference in the two equations is that minimum value in the radiograph occurs where the x-rays travel the longest path through the object, namely, along the diameter. In the peak image, the minimum value occurs near the edges

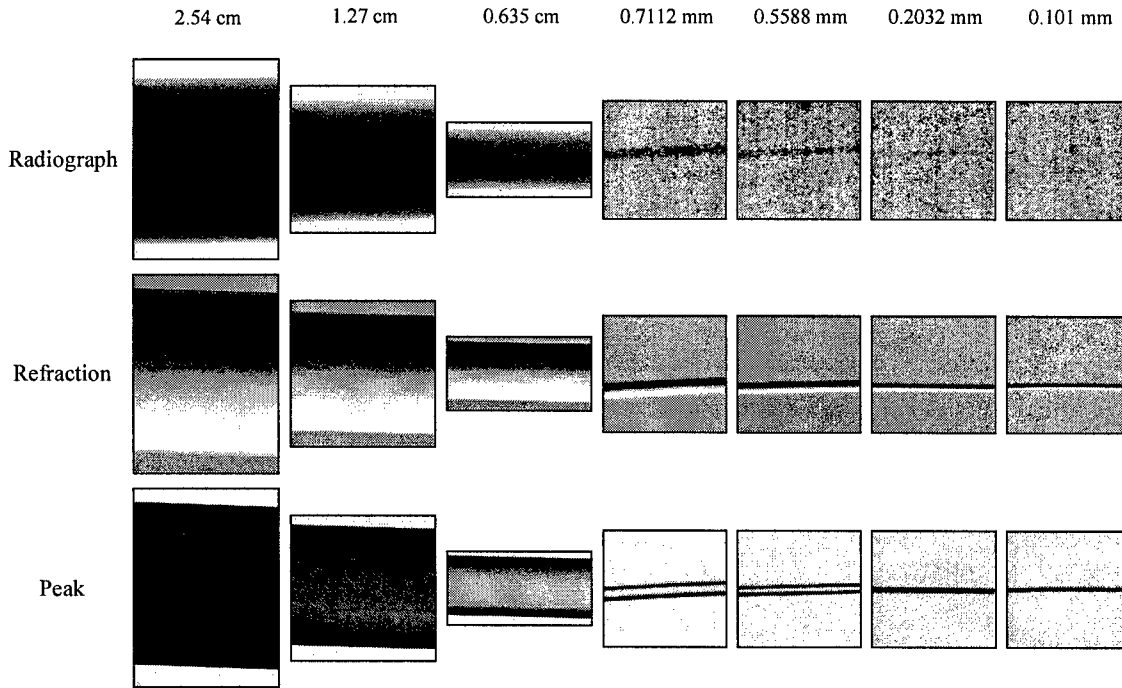


Figure 3. Comparison of DEI images to conventional radiographs. Radiographs of the images are in the top row, while the refraction images are in the second row and the peak images are in the bottom row. The diameters of the objects are given across the top. The first three images in each row are of the Lucite cylinders, while the last four in each row are of the Nylon wires.

of the object, where the x-rays have traveled the shortest path, but have also undergone the greatest amount of refraction.

In addition to the definition of contrast, signal-to-noise ratios (SNR) have been defined for both the refraction image as well as the radiographic image. The SNR in the refraction image is given by

$$SNR_{ref} = \frac{R_{max} - R_{min}}{\sigma_{avg}}, \quad (4)$$

where R_{max} and R_{min} are the maximum and minimum values in the refraction image, and σ_{avg} is the noise level in the background. The noise has been defined as one standard deviation from the mean. Similarly, the SNR for the radiograph is given by,

$$SNR_{rad} = \frac{I_{avg} - I_{min}}{\sigma_{avg}}, \quad (5)$$

where all the terms are defined above

In comparing the DEI results to the radiographic results, a quantity, called the gain value is defined. For the peak image, the gain is obtained by taking the ratio of the peak contrast to the radiographic contrast:

$$G_{peak} = \frac{C_{peak}}{C_{rad}}, \quad (6)$$

while for the refraction image, the gain is obtained by taking the ratio of the refraction SNR to the radiographic SNR, or,

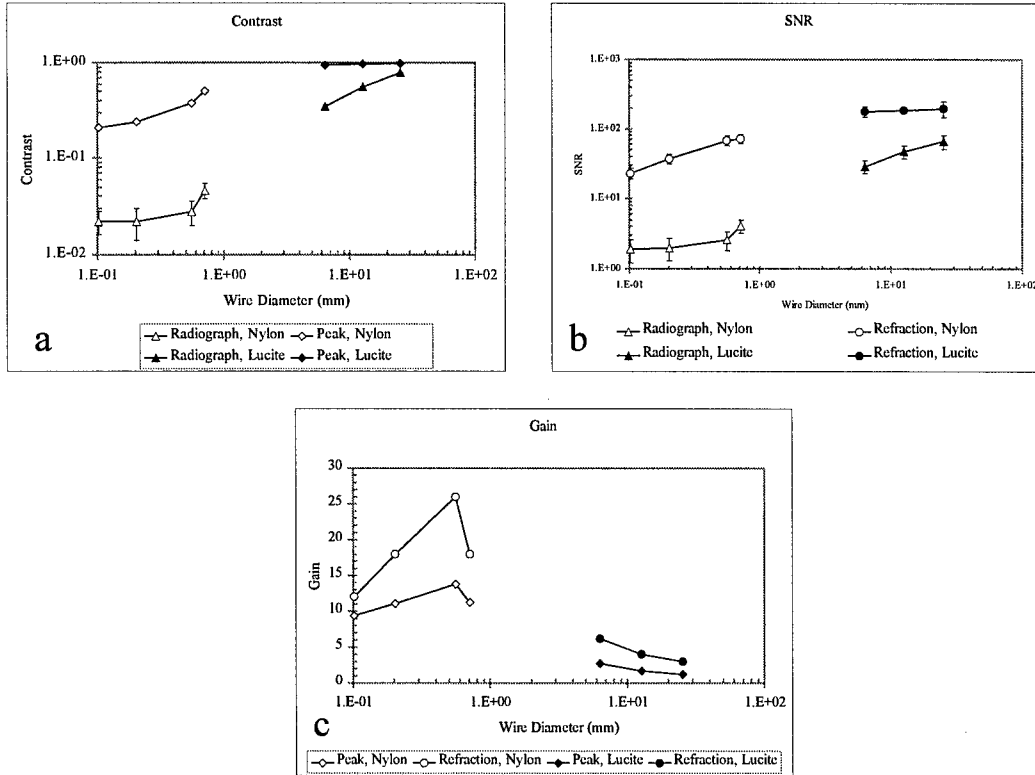


Figure 4. Experimental results. For all plots, results of the Nylon wires are empty symbols, while the Lucite cylinders are denoted by filled symbols. a) Comparison of peak contrast to radiographic contrast. b) Comparison of refraction SNR to radiographic SNR. c) Comparison of refraction gain to peak gain. Error bars indicate one standard deviation from the mean value.

$$G_{ref} = \frac{SNR_{ref}}{SNR_{rad}}. \quad (7)$$

Figure 4 shows the experimental results. Each graph plots the contrast, SNR, or gain as a function of object diameter. From 4a and 4b the results clearly show that both the peak contrast and refraction SNR are much higher at all diameters than their radiographic counterparts, with the largest differences occurring at the smaller diameters. As for the gain values, there is a peak in both plots near 0.7-mm diameter. This suggests that as the object size approaches pixel dimensions, the contrast becomes dominated by extinction (a combination of absorption and ultra-small angle scattering). Indeed, a pixel-sized object will show only extinctive effects.

Figure 5 shows the results of computer simulations for Nylon wires of varying diameter. For this particular simulation, the detector was similar to the Fuji system, except that it lacked the same noise characteristics. Therefore, these results cannot be directly compared to the results in figure 4. Each graph plots the contrast, SNR, or gain as a function of object diameter, as in figure 4. In this case, however, the plots are all for Nylon. A few artifacts are present in the plots in the small diameter range. These are due to computational techniques, which are undergoing refinement. But the trends are clearly similar to the experimental results, including the local maximum in the gain values. There is a much sharper decline in all plots in the small diameter regime, unlike in figure 4. This also indicates the domination of extinction over refraction at small diameters. The sharp decline is attributed to the low noise level in the simulation. Simulations using higher noise levels suggest a more gradual decline.

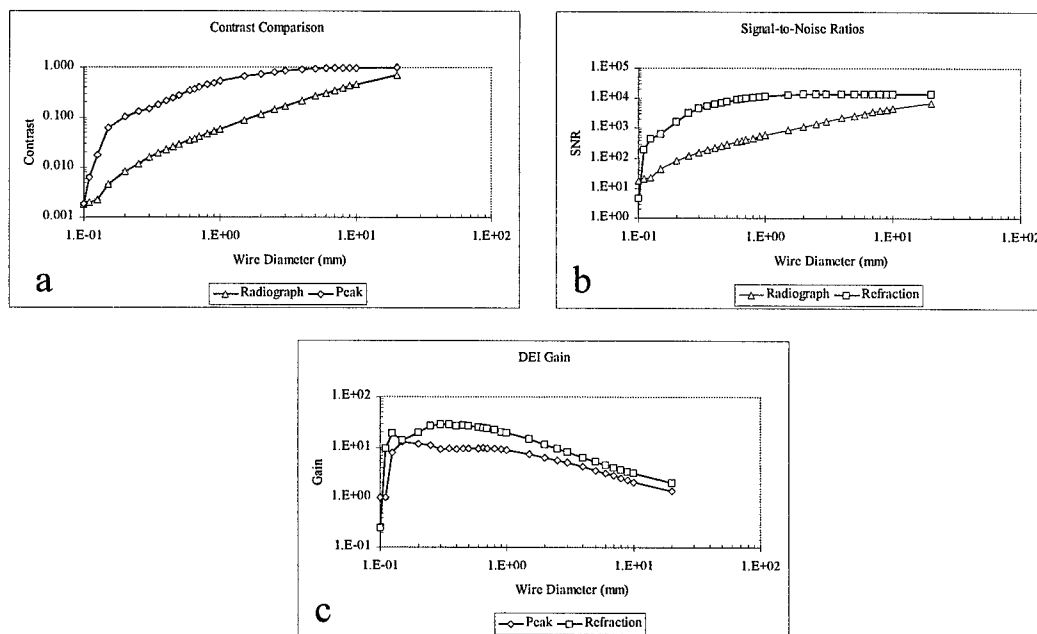


Figure 5. Results of computer simulations for nylon wires of varying diameter. Simulations assume a detector similar to the Fuji system with similar PSF characteristics. Source characteristics are similar to the X-15A beamline at NSLS.

Training Accomplishments

As a result of the efforts of the past year, a great deal of training value has been gained. Expertise in conducting DEI experiments and proficiency of synchrotron beamline operations have been achieved. These skills have been useful in developing a doctoral dissertation and in training individuals joining the DEI collaboration. The project has also generated new image processing techniques and has resulted in the improvement of existing ones. This is important because DEI is still a relatively new imaging modality. These new techniques will prove invaluable to future researchers as the technique is implemented in the clinic. In addition to practical experience, formal coursework in scanning electron microscopy has supplemented a firm foundation in analytical imaging techniques. Finally, by conducting experiments on objects with a simple geometry, it is now possible to apply these experiments and techniques to objects of greater importance, namely, calcifications in breast tissue.

Key Research Accomplishments

- Developed a method for quantifying contrast in images obtained using DEI
- Compared DEI contrasts to conventional radiographic contrast and demonstrated the superiority of DEI over conventional radiography with respect to contrast enhancement
- Developed computational techniques for modeling DEI images and for predicting image contrast, especially at near-pixel-sized objects

Reportable Outcomes

- A poster on this study was given at the 12th National Synchrotron Radiation Instrumentation Conference, August 22 - 24, 2001, Madison, Wisconsin

- A presentation including this study was given at the American Physical Society Annual Meeting, March 12 – 16, 2001, Seattle, Washington
- It is intended that the results of this work will be submitted for publication

Conclusions

This findings in this study clearly demonstrate the ability of DEI to produce higher contrast images when compared with conventional radiographs. This is true even as the object size is approaches the size of a detector pixel (or its PSF). Conventional radiographic contrast suffers in this regime more than enhanced contrast. This becomes important for determining an optimal detector for a clinical DEI device. Smaller pixels in a detector may improve resolution and reduce aliasing, but noise levels will increase, limiting the minimum size of an object that can be resolved. Future investigations will include computer modeling of images using a variety of detector characteristics and conducting experiments on calcifications embedded in breast tissue. The latter will pose an interesting challenge because calcifications are not typically homogeneous in composition like the objects used in this study. Their extinction characteristics are considerably different and pixel-sized or near-pixel-sized calcifications will require additional image processing techniques to illustrate the improved contrast using DEI.

References

1. Chapman D., Thomlinson W., Johnston R.E., Washburn D., Pisano E., Gmur N., Zhong Z., Menk R., Arfelli F., and Sayers D., "Diffraction Enhanced x-ray Imaging," *Phys. Med. Biol.* **42** (1997) 2015-2025.
2. Pisano E.D., Johnston R.E., Chapman D., Geradts J., Iacocca M., Livasy C.A., Washburn D.B., Sayers D.E., Zhong Z., Kiss M.Z., Thomlinson W.C., "Human Breast Cancer Specimens: Diffraction Enhanced Imaging with Histologic Correlation – Improved Conspicuity of Lesion Detail Compared with Digital Radiography," *Radiology* **214** (2000) 895-901.
3. Zhong Z., Thomlinson W., Chapman D., Sayers D., "Implementation of Diffraction Enhanced Imaging Experiments at the NSLS and APS," *Nucl. Instr. and Meth. A*, **450** (2000) 556-567.
4. Colonna S., D'Acapito F., Mobilio S., Onori S., Pugliani L., Romanzetti S., Rustichelli F., "Curved Optics for x-ray phase contrast imaging by synchrotron radiation," *Phys. Med. Biol.* **46** (2001) 967-974.
5. Kotre CJ, Birch IP, "Phase contrast enhancement of x-ray mammography: a design study," *Phys. Med. Biol.* (1999) 2853 – 2866.
6. Ingal VN, Beliaevskaya EA, Brianskaya AP, Merkurieva RD, "Phase mammography – a new technique for breast investigation," *Phys. Med. Biol.* (1998) 2555 – 2567.



Record Retrieved

[HOME](#) [SEARCH](#) [INFO](#) [MAP](#) [?](#)

Document Title : Integration of Digital Detectors into a Diffraction Enhanced Imaging System

Filename	MIME Type	Size (Bytes)
ADB282896.pdf	application/pdf	673222

[<-- Previous Hit](#)

(This is hit 2 of 4.)

[Next Hit -->](#)

Please make correction

AD Number: ADB282896

Subject Categories: COMPUTER PROGRAMMING AND SOFTWARE MEDICINE AND MEDICAL RESEARCH

Corporate Author: NORTH CAROLINA STATE UNIV AT RALEIGH

Title: Integration of Digital Detectors into a Diffraction Enhanced Imaging System

Descriptive Note: Annual summary 1 Aug 2000-31 Jul 2001

Personal Authors: ~~Gayers, Dale~~ *Kiss, miklos ; Sayers, Dale*

Report Date: AUG 2001

Pages: 11 PAGES

Contract Number: **DAMD17-99-1-9329**

Monitor Acronym: XA

Monitor Series: USAMRMC

Limitations: Distribution authorized to U.S. Gov't. agencies only; Proprietary Info.; Aug 2001. Other requests shall be referred to U.S. Army Medical Research and Materiel Command, 504 Scott St., Ft. Detrick, MD 21702-5012.

Descriptors: *COMPUTERIZED SIMULATION, *DIGITAL SYSTEMS, *RADIOGRAPHY, PEAK VALUES, RATIOS, CONTRAST, DETECTORS, WIRE, NYLON, PATHS, POLYMETHYL METHACRYLATE, CRYSTALS, LIGHT SOURCES, INTEGRATION, CYLINDRICAL BODIES, SILICON, IMAGES, GAIN, VALUE, REFRACTION, ANALYZERS, SYNCHROTRONS.

Abstract: Refraction contrast of cylindrical objects have been obtained using Diffraction Enhanced Imaging (DEI) and compared to the conventional radiographic contrast. Lucite cylinders and nylon wires were imaged using 18 kev synchrotron radiation at the National Synchrotron Light Source (NSLS) at Brookhaven National Laboratory. The DEI images were obtained by placing a Silicon analyzer crystal tuned to the 333 plane in the beam path between the sample and the detector. They showed improved contrast of the objects when compared to normal radiographs. This comparison, called the gain value, is the ratio of the refraction contrast (or peak contrast) to the conventional radiographic contrast. Experiments and computer simulation consistently resulted of gain values larger than one, indicating improved contrast due to DEI. Experimental results and corresponding computer simulations are presented.

Limitation Code: U.S. GOVT. ONLY; DOD CONTROLLED

Source Code: 259300

Citation Creation Date: 23 OCT 2002



DEPARTMENT OF THE ARMY
US ARMY MEDICAL RESEARCH AND MATERIEL COMMAND
504 SCOTT STREET
FORT DETRICK, MARYLAND 21702-5012

REPLY TO
ATTENTION OF:

MCMR-RMI-S (70-1y)

28 July 03

MEMORANDUM FOR Administrator, Defense Technical Information
Center (DTIC-OCA), 8725 John J. Kingman Road, Fort Belvoir,
VA 22060-6218

SUBJECT: Request Change in Distribution Statement

1. The U.S. Army Medical Research and Materiel Command has reexamined the need for the limitation assigned to technical reports written for this Command. Request the limited distribution statement for the enclosed accession numbers be changed to "Approved for public release; distribution unlimited." These reports should be released to the National Technical Information Service.

2. Point of contact for this request is Ms. Kristin Morrow at DSN 343-7327 or by e-mail at Kristin.Morrow@det.amedd.army.mil.

FOR THE COMMANDER:

Encl

PHYLLIS M. RINEHART

Deputy Chief of Staff for
Information Management

ADB233865	ADB264750
ADB265530	ADB282776
ADB244706	ADB286264
ADB285843	ADB260563
ADB240902	ADB277918
ADB264038	ADB286365
ADB285885	ADB275327
ADB274458	ADB286736
ADB285735	ADB286137
ADB286597	ADB286146
ADB285707	ADB286100
ADB274521	ADB286266
ADB259955	ADB286308
ADB274793	ADB285832
ADB285914	
ADB260288	
ADB254419	
ADB282347	
ADB286860	
ADB262052	
ADB286348	
ADB264839	
ADB275123	
ADB286590	
ADB264002	
ADB281670	
ADB281622	
ADB263720	
ADB285876	
ADB262660	
ADB282191	
ADB283518	
ADB285797	
ADB269339	
ADB264584	
ADB282777	
ADB286185	
ADB262261	
ADB282896	
ADB286247	
ADB286127	
ADB274629	
ADB284370	
ADB264652	
ADB281790	
ADB286578	